Surface transfer doping of diamond by MoO3: A combined spectroscopic and Hall measurement study

ARTICLE *in* APPLIED PHYSICS LETTERS · NOVEMBER 2013

Impact Factor: 3.3 · DOI: 10.1063/1.4832455

Surface transfer doping of diamond by MoO3: A combined spectroscopic and Hall measurement study

Stephen A. O. Russell, Liang Cao, Dongchen Qi, Alexandre Tallaire, Kevin G. Crawford et al.

Citation: Appl. Phys. Lett. **103**, 202112 (2013); doi: 10.1063/1.4832455
View online: http://dx.doi.org/10.1063/1.4832455
View Table of Contents: http://apl.aip.org/resource/1/APPLAB/v103/i20
Published by the AIP Publishing LLC.

Surface transfer doping of diamond by MoO_3: A combined spectroscopic and Hall measurement study

Stephen A. O. Russell,[1,a)] Liang Cao,[2] Dongchen Qi,[3,b)] Alexandre Tallaire,[4] Kevin G. Crawford,[1] Andrew T. S. Wee,[5] and David A. J. Moran[1]
[1]*School of Engineering, University of Glasgow, Glasgow G12 8LT, United Kingdom*
[2]*Department of Chemistry, National University of Singapore, Singapore 117543, Singapore*
[3]*Department of Physics, La Trobe University, Victoria 3086, Australia*
[4]*LSPM-CNRS, Université Paris 13, Villetaneuse 93430, France*
[5]*Department of Physics, National University of Singapore, Singapore 117542, Singapore*

(Received 23 September 2013; accepted 4 November 2013; published online 14 November 2013)

Surface transfer doping of diamond has been demonstrated using MoO_3 as a surface electron acceptor material. Synchrotron-based high resolution photoemission spectroscopy reveals that electrons are transferred from the diamond surface to MoO_3, leading to the formation of a sub-surface quasi 2-dimensional hole gas within the diamond. *Ex-situ* electrical characterization demonstrated an increase in hole carrier concentration from $1.00 \times 10^{13}/cm^2$ for the air-exposed hydrogen-terminated diamond surface to $2.16 \times 10^{13}/cm^2$ following MoO_3 deposition. This demonstrates the potential to improve the stability and performance of hydrogen-terminated diamond electronic devices through the incorporation of high electron affinity transition metal oxides. © *2013 AIP Publishing LLC*. [http://dx.doi.org/10.1063/1.4832455]

Diamond is considered an attractive semiconductor material for high power/high frequency electronic devices due to its high intrinsic breakdown field of 10 MV/cm, thermal conductivity >20 W/cm K, and band gap of 5.47 eV.[1] Promising high-frequency performance has already been demonstrated for hydrogen-terminated diamond surface channel field effect transistors (FETs)[2,3] with a cutoff frequency (f_T) of 53 GHz recently reported.[4] Due to the substantial challenges that still remain with substitutional doping processes in diamond,[5] these devices utilize the sub-surface conductivity of hydrogen-terminated diamond induced by surface transfer doping as an alternative doping strategy. This process relies on the exchange of interfacial charge between the diamond valence band and the energetically accessible energy states of atmospheric molecules on the diamond surface.[6] Although this doping technique has produced the highest performance diamond FETs to date, the volatility of the atmospheric adsorbates (upon which this process typically relies) results in instability of electronic device operation.[7] Recent studies have shown that molecules with high electron affinity such as C_{60}, $C_{60}F_{xx}$, and F_4-TCNQ may be deposited on to the hydrogen-terminated diamond surface to replace the atmospheric adsorbate layer and instigate surface transfer doping.[5,8–10] The incorporation of a barrier layer such as ZnTPP to prevent the atmospheric induced doping has also been demonstrated.[11] While these organic molecules present an alternative route to surface transfer doping in diamond, they do not necessarily provide sufficient stability of operation for hydrogen-terminated diamond electronic devices when exposed to atmosphere or varying temperature environments. For example, it has been shown that C_{60} molecules will sublimate from the hydrogen-terminated diamond surface at ~200 °C,[12] limiting their application in the development of a robust device technology. More recent work however has also demonstrated improved stability of hydrogen-terminated diamond FETs through exposure of the surface to NO_2 prior to encapsulation with Al_2O_3.[13]

In this work, we present MoO_3 as a surface acceptor material for surface transfer doping in diamond with the potential to provide improved device performance and robustness of operation. Owing to its very high work function, MoO_3 has been routinely adopted as an anode buffer layer to greatly enhance the hole injection/extraction in organic electronic devices, or as a bulk *p*-type dopant for organic wide band gap materials.[14–16] Recent electrical transport measurements have also confirmed the non-destructive *p*-type surface transfer doping of graphene utilizing MoO_3,[17] with the many superior electronic properties of graphene unperturbed.[18] With an electron affinity of 6.7 eV,[19] the conduction band minimum of MoO_3 lies more than 2.8 eV below the hydrogen-terminated diamond valence band maximum, making electron transfer from the diamond to MoO_3 energetically favorable as shown in Figure 1.

To investigate this surface transfer doping process utilizing MoO_3 on hydrogen-terminated diamond, two 4.7 × 4.7 mm chemical vapor deposition (CVD) single-crystal (001) diamond samples provided by Element Six were used in this study.

Sample I: Photoemission spectroscopy (PES) test sample—A 300 nm-thick boron-doped epitaxial layer was grown on sample I by microwave plasma assisted CVD in a bell-jar reactor using a pressure of 220 mbar, a microwave power of 3100 W, and a CH_4 concentration of 4% in H_2. The chamber of this reactor is dedicated to the growth of heavily doped thick films with high boron background.[20] No addition of diborane (B_2H_6) therefore was required to reach a doping level as high as $10^{18}/cm^3$ in the deposited diamond film. The resulting moderate conductivity allowed synchrotron based photoemission spectroscopy (PES) measurements to

a)Electronic mail: Stephen.Russell@glasgow.ac.uk.
b)Electronic mail: D.Qi@latrobe.edu.au.

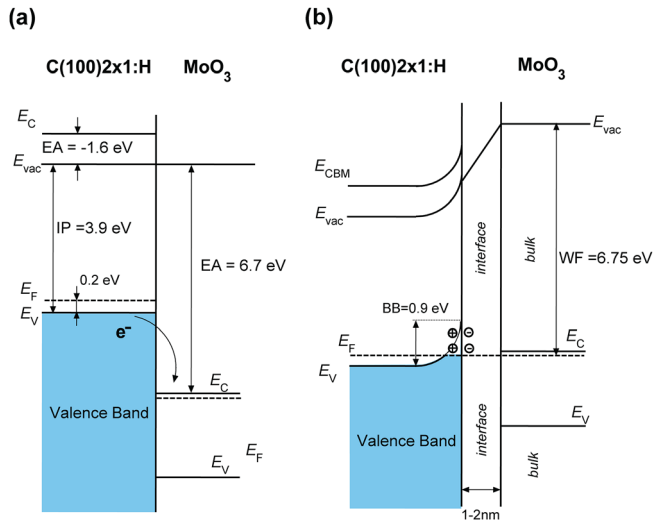

FIG. 1. Energy band diagram showing the surface transfer doping process in hydrogen-terminated diamond using MoO_3 as a surface acceptor. The energy levels are measured by PES and the detailed procedure used for this process is described elsewhere.[9] In the energy band diagram, IP represents ionization potential, EA represents electron affinity, and WF represents work function.

be conducted on the diamond surface without any charging effects. Prior to the PES measurements, the diamond sample was cleaned thoroughly in aqua regia (HNO_3:HCl = 1:3) followed by piranha (H_2O_2:H_2SO_4 = 1:3) with both heated to 70 °C to remove any metallic and organic adsorbates. The sample was then introduced to a microwave hydrogen plasma chamber to obtain a hydrogen-terminated 2×1 reconstructed (001) surface. The hydrogen plasma treatment was performed at the microwave power of 1000 W, 30 Torr hydrogen pressure, and 300 SCCM of hydrogen gas flow with diamond heated around 800–1000 °C for 15 min in a 2.45 GHz microwave plasma reactor (Astex). After the hydrogen plasma treatment, the diamond sample was transferred into an ultra-high vacuum (UHV) chamber with a base pressure of 1×10^{-10} mbar at the end-station of SINS beamline at the Singapore Synchrotron Light Source (SSLS) for synchrotron characterization.[21] It was then annealed *in-situ* at 400 °C to remove any residual surface adsorbates and/or remnant hydrocarbon molecules from the hydrogen plasma process, whilst leaving the hydrogen termination intact.[12,22] After cooling-down to room temperature, the deposition of MoO_3 was carried out by subliming from a standard Knudsen-cell set at 437 °C. The nominal thickness of MoO_3 thin films was estimated from the attenuation of the bulk diamond C 1*s* peak intensity after each deposition.

PES spectra were recorded by a Scienta R4000 electron energy analyzer at normal emission geometry. The binding energies of all PES spectra were calibrated and referenced to the Fermi energy of a sputtered gold foil in electrical contact with the diamond sample. The work function was measured by recording the secondary electron emission in low kinetic energy region with incoming photon energy set to 60 eV. A −9 V bias was applied to the sample in order to overcome the work function of the analyzer.

The surface transfer doping process at the MoO_3/intrinsic diamond interface was monitored by photoemission spectroscopy as a function of MoO_3 coverage (Figure 2). Immediately after the deposition of 1 Å MoO_3, a substantial reduction as large as 0.40 eV in the binding energy of the diamond C 1*s* peak is observed (Figure 2(a)). The diamond peak continues to shift to the lower binding energy side with subsequent MoO_3 deposition, and becomes almost unchanged with MoO_3 coverage beyond 16 Å as also shown in Figure 2(c). The total binding energy shift as a result of MoO_3 deposition is 0.90 eV. Owing to the extremely high surface sensitivity of the C 1*s* PES spectra achieved by the incident photon energy of 350 eV, only the very surface region of diamond is probed. Consequently, the measured diamond C 1*s* peak binding energy directly indicates the relative position of the Fermi energy with respect to the diamond energy levels on the surface after electrostatic equilibrium is established. The observed reduction in the C 1*s* binding energy, therefore, agrees with an upward band bending of the same amount towards the diamond surface, suggesting significant hole accumulation in the diamond surface region as a result of the

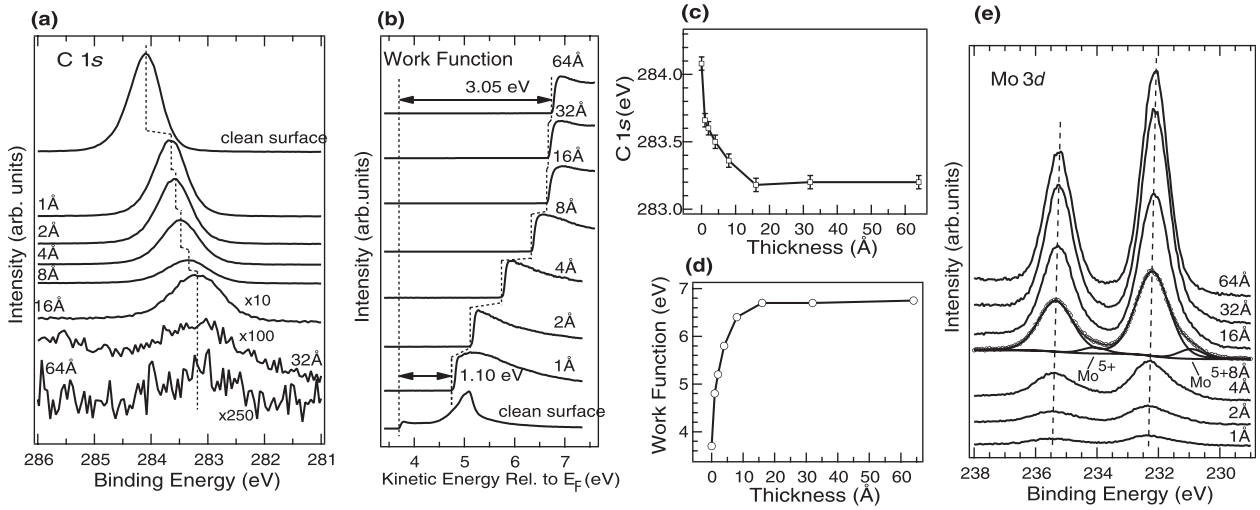

FIG. 2. (a) PES core level spectra of C1*s* with photon energy of 350 eV. (b) Secondary electron emission cut-off with photon energy of 60 eV for hydrogen-terminated diamond with increasing MoO_3 coverage. The diamond C 1*s* peak position and work function value (extracted from the cut-off position in (b) as a function of MoO_3 coverage are plotted in (c) and (d), respectively. (e) PES core level spectra of Mo 3*d* with photon energy of 350 eV. An example of the least square peak fitting for the Mo 3*d* peaks is shown for 4 Å coverage of MoO_3.

surface transfer doping effect of MoO_3 as demonstrated in Figure 1. Similar behavior in the diamond C 1*s* peak has also been observed for other surface acceptors such as F_4-TCNQ,[5,9] C_{60},[23] and $C_{60}F_{48}$,[10] and usually are considered as direct evidence of effective surface transfer doping. Moreover, similar to the observation of negatively charged surface acceptor species for F_4-TCNQ and $C_{60}F_{48}$ on diamond as a result of the surface transfer doping process, negatively charged MoO_3 interfacial clusters are also recognized in the Mo 3*d* spectra by performing least-square peak fitting (Figure 2(e)). The Mo^{5+}/Mo^{6+} ratio is found to be reduced significantly from 0.1 for 1 Å coverage to less than 0.02 for 64 Å coverage, consistent with the interfacial nature of the negatively charged MoO_3 species.

The charge separation across the diamond/MoO_3 interface (i.e., positive charge on diamond side and negative charge on MoO_3 side) undoubtedly manifests itself as the formation of an interface dipole[5,9] as revealed by the significant increase in work function from 3.70 eV in the clean diamond surface to 6.75 eV in the thick MoO_3 overlayers (indicated by the cut-off position in Figure 2(b)). A total work function change of 3.05 eV after MoO_3 deposition is observed (also see Figure 2(d)), which is larger than that induced by any previously reported surface acceptors on diamond, corroborating the extraordinary surface transfer doping capability offered by MoO_3.

Sample II: Hall electrical characterization test sample—In contrast to sample I, which incorporated a boron-doped surface layer to minimize charging effects during PES measurement, the surface of the intrinsic diamond substrate following hydrogen termination was utilized on sample II for electrical characterization and *ex-situ* verification of surface transfer doping using MoO_3. Prior to hydrogen-termination, an acid based clean similar to that described for sample I was performed. Hydrogen-termination was then undertaken in a high-power hydrogen plasma for 30 min at a substrate temperature of 580 °C. Van der Pauw (VDP) test structures were then fabricated to extract Hall measurement data and investigate the electrical transport properties of the resultant hole carriers within the diamond. The fabrication process used to create the VDP structures is shown in Figure 3 and is described below.

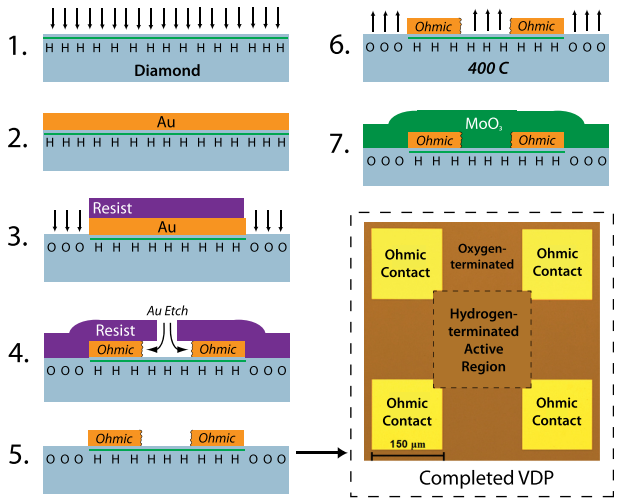

FIG. 3. Fabrication process for Van der Pauw Hall measurement structures: 1. Diamond surface hydrogen-termination, 2. deposition of 80 nm thick Au layer, 3. electrical isolation via Au etch and O_2 plasma, 4. Au etch for VDP 'active' region and ohmic contact formation, 5. completed VDP structure, 6. *In-situ* 400 °C anneal, and 7. deposition of 100 nm thick MoO_3 layer.

An 80 nm thick Au film was initially deposited via electron-beam evaporation onto the hydrogen-terminated diamond surface to protect it during processing and to form ohmic contacts to the sub-surface hole layer. A PMMA resist mask was patterned by electron-beam lithography and the geometry of the VDP structure electrically isolated by selectively removing the Au layer using a KI/I_2 based wet etch then treating the exposed diamond surface with oxygen plasma. A second stage of lithography and wet etch was then performed to remove the Au in the remaining hydrogen-terminated VDP "active" region (as indicated by step 4 in Figure 3) and to form the ohmic contacts directly from the remaining Au layer. The sample was then transferred in to a thermal evaporator and a 400 °C anneal performed for 15 min at a chamber pressure $<1 \times 10^{-7}$ Torr to ensure removal of any residual adsorbates from the diamond surface.[12,22] Finally, a 100 nm thick MoO_3 layer was deposited across the diamond surface by thermal evaporation without exposing the sample to atmosphere following the *in-situ* 400 °C anneal.

Ex-situ Hall measurement of the VDP structures was performed using a Nanometrics HL5500 Hall measurement system immediately prior to (between steps 5 and 6 in Figure 3) and after the annealing and MoO_3 deposition stages (after step 7 in Figure 3). Values for the sheet resistance, hole mobility, and carrier concentration were extracted from this process and are presented in Table I.

Prior to MoO_3 deposition, Hall measurement yields charge transport values typically reported for hydrogen-terminated diamond exposed to atmosphere.[24] Immediately following deposition of MoO_3, the hole concentration is increased from $1 \times 10^{13}/cm^2$ to $2.16 \times 10^{13}/cm^2$ and the mobility reduced from 69 cm^2/V s to ~51 cm^2/V s, verifying the formation of a sub-surface hole layer within the diamond after MoO_3 deposition. The increase in hole concentration may be attributed to the transfer of a higher density of electrons from the diamond valence band to the MoO_3 layer, leading to an enhanced surface transfer doping effect in comparison with that achieved with the atmosphere-exposed diamond surface. The exact mechanism by which the hole mobility is reduced is not yet fully understood, but may be related to reduced proximity between the 2-dimensional hole layer and diamond surface due to increased bending of the diamond valence band maximum

TABLE I. *Ex-situ* VDP measurements prior to and post MoO_3 deposition.

	Sheet resistance (kΩ/sq.)	Mobility (cm^2/V s)	Sheet carrier concentration ($\times 10^{13}/cm^2$)
Before MoO_3 deposition	9.1	69.0	1.00
Immediately after MoO_3 deposition	5.6	51.2	2.16
Change	−38%	−26%	+116%
4 h after MoO_3 deposition	5.6	51.5	2.15

when in contact with the MoO_3 layer. Despite the modest decrease in hole mobility, the resultant substantial increase in carrier concentration leads to an overall reduction in sheet resistance from 9.1 kΩ/sq. to 5.6 kΩ/sq.

Previous work has demonstrated modification to the electronic structure of MoO_3 layers when exposed to atmosphere.[25] To monitor the short term stability of the electrical test sample, Hall measurements were therefore taken again after the sample was exposed to atmosphere for 4 h. Minimal variation in the extracted values were observed over this timescale (as shown in Table I). This may in part be attributed to the use of a 100 nm thick film of MoO_3, thus reducing the rate of degradation in comparison with that observed for thinner layers. Further work will be required to characterize the long term stability of these layers on hydrogen-terminated diamond. Furthermore, to ensure these results were indicative of hole transport solely through the diamond, and to eliminate the possibility of parallel conduction through the deposited MoO_3 film, the conductivity of an identical (i.e. 100 nm thick) MoO_3 layer deposited onto an insulating SiO_2 control sample was measured. This process demonstrated negligible conduction through the MoO_3, with no measurable current above the noise floor of the measurement system (~100 nA) observed.

In conclusion, MoO_3 has been used to demonstrate surface transfer doping on hydrogen-terminated diamond. This was verified experimentally using photoemission spectroscopy, with the largest total work function shift yet reported for a surface acceptor material on diamond observed. Hall measurement data further confirmed the onset of surface transfer doping using MoO_3 and demonstrated a substantial increase in hole carrier concentration in comparison with atmosphere exposed hydrogen-terminated diamond. These results indicate a route to improve both the stability and performance of future hydrogen-terminated diamond devices through the use of MoO_3 as a robust and high doping efficiency surface acceptor material.

The authors wish to thank the staff at the James Watt Nanofabrication Centre for their assistance with this work and Element Six Ltd. and Diamond Microwave Devices Ltd. for diamond material supply.

[1]C. J. H. Wort and R. S. Balmer, Mater. Today **11**, 22 (2008).
[2]K. Hirama, H. Takayanagi, S. Yamauchi, Y. Jingu, H. Umezawa, and H. Kawarada, in *IEDM Technical Digest* (2007), p. 873.
[3]K. Ueda, M. Kasu, Y. Yamauchi, T. Makimoto, M. Schwitters, D. J. Twitchen, G. A. Scarsbrook, and S. E. Coe, IEEE Electron Device. Lett. **27**, 570 (2006).
[4]S. A. O. Russell, S. Sharabi, A. Tallaire, and D. A. J. Moran, IEEE Electron Device Lett. **33**, 1471 (2012).
[5]W. Chen, D. Qi, X. Gao, and A. T. S. Wee, Prog. Surf. Sci. **84**, 279 (2009).
[6]F. Maier, M. Riedel, B. Mantel, J. Ristein, and L. Ley, Phys. Rev. Lett. **85**, 3472 (2000).
[7]M. Kasu, K. Ueda, Y. Yamauchi, A. Tallaire, and T. Makimoto, Diamond Relat. Mater. **16**, 1010 (2007).
[8]P. Strobel, M. Riedel, J. Ristein, and L. Ley, Nature **430**, 439 (2004).
[9]D. Qi, W. Chen, X. Gao, L. Wang, S. Chen, K. P. Loh, and A. T. S. Wee, J. Am. Chem. Soc. **129**, 8084 (2007).
[10]M. T. Edmonds, M. Wanke, A. Tadich, H. M. Vulling, K. J. Rietwyk, P. L. Sharp, C. B. Stark, Y. Smets, A. Schenk, Q.-H. Wu, L. Ley, and C. I. Pakes, J. Chem. Phys. **136**, 124701 (2012).
[11]D. P. Langley, Y. Smets, C. B. Stark, M. T. Edmonds, A. Tadich, K. J. Rietwyk, A. Schenk, M. Wanke, Q.-H. Wu, P. J. Barnard, L. Ley, and C. I. Pakes, Appl. Phys. Lett. **100**, 032103 (2012).
[12]L. Ley, J. Ristein, F. Meier, M. Riedel, and P. Strobel, Physica B **376–377**, 262 (2006).
[13]K. Hirama, H. Sato, Y. Harada, H. Yamamoto, and M. Kasu, IEEE Electron Device Lett. **33**, 1111 (2012).
[14]S. Murase and Y. Yang, Adv. Mater. **24**, 2459 (2012).
[15]M. Kröger, S. Hamwi, J. Meyer, T. Riedl, W. Kowalsky, and A. Kahn, Org. Electron. **10**, 932 (2009).
[16]S. D. Ha, J. Meyer, and A. Kahn, Phys. Rev. B **82**, 155434 (2010).
[17]Z. Chen, I. Santoso, R. Wang, L. F. Xie, H. Y. Mao, H. Huang, Y. Z. Wang, X. Y. Gao, Z. K. Chen, D. Ma, A. T. S. Wee, and W. Chen, Appl. Phys. Lett. **96**, 213104 (2010).
[18]L. Xie, X. Wang, H. Mao, R. Wang, M. Ding, Y. Wang, B. Özyilmaz, K. P. Loh, A. T. S. Wee, Ariando, and W. Chen, Appl. Phys. Lett. **99**, 012112 (2011).
[19]M. T. Grenier, M. G. Helander, W.-M. Tang, Z.-B. Wang, J. Qiu, and Z.-H. Lu, Nature Mater. **11**, 76 (2012).
[20]R. Issaoui, J. Achard, A. Tallaire, F. Silva, A. Gicquel, R. Bisaro, B. Servet, G. Garry, and J. Barjon, Appl. Phys. Lett. **100**, 122109 (2012).
[21]X. Yu, O. Wilhelmi, H. O. Moser, S. V. Vidyaraj, X. Gao, A. T. S. Wee, T. Nyunt, H. Qian, and H. Zheng, J. Electron Spectrosc. Relat. Phenom. **144–147**, 1031 (2005).
[22]D. Qi, J. Sun, X. Gao, L. Wang, S. Chen, K. P. Loh, and A. T. S. Wee, Langmuir **26**, 165 (2010).
[23]P. Strobel, M. Riedel, J. Ristein, L. Ley, and O. Boltalina, Diamond Relat. Mater. **14**, 451 (2005).
[24]A. Aleksov, M. Kubovic, M. Kasu, P. Schmidt, D. Grobe, S. Ertl, M. Schreck, B. Stritzker, and E. Kohn, Diamond Relat. Mater. **13**, 233 (2004).
[25]J. Meyer, A. Shu, M. Kröger, and A. Kahn, Appl. Phys. Lett. **96**, 133308 (2010).